DOI: 10.1002/chem.200801073

# Comparative Analysis of Electron-Density and Electron-Localization Function for Dinuclear Manganese Complexes with Bridging Boron- and Carbon-Centered Ligands

**Kathrin Götz,[a] Martin Kaupp,*[a] Holger Braunschweig,[a] and Dietmar Stalke[b]**

*Dedicated to Professor Werner Kutzelnigg on the occasion of his 75th birthday*

**Abstract:** Bonding in borylene-, carbene-, and vinylidene-bridged dinuclear manganese complexes $[MnCp(CO)_2]_2X$ (X = B-*t*Bu, B = $NMe_2$, $CH_2$, C=$CH_2$) has been compared by analyses based on quantum theory of atoms in molecules (QTAIM), on the electron-localization function (ELF), and by natural-population analyses. All of the density functional theory based analyses agree on the absence of a significant direct Mn–Mn bond in these complexes and confirm a dominance of delocalized bonding via the bridging ligand. Interestingly, however, the topology of both charge density and ELF related to the Mn-bridge-Mn bonding depend qualitatively on the chosen density functional (except for the methylene-bridged complex, which exhibits only one three-center-bonding attractor both in $-\nabla^2\rho$ and in ELF). While gradient-corrected functionals provide a picture with localized two-center X–Mn bonding, increasing exact-exchange admixture in hybrid functionals concentrates charge below the bridging atom and suggests a three-center bonding situation. For example, the bridging boron ligands may be described either as substituted boranes (e.g., at BLYP or BP86 levels) or as true bridging borylenes (e.g., at BHLYP level). This dependence on the theoretical level appears to derive from a bifurcation between two different bonding situations and is discussed in terms of charge transfer between X and Mn, and in the context of self-interaction errors exhibited by popular functionals.

**Keywords:** bond theory · electron localization function · manganese · metal–metal bonding · quantum theory

## Introduction

Boron chemistry is renowned for its interesting and peculiar bonding patterns related to electron deficiency and high Lewis acidity. These characteristics of boron compounds distinguish them also as suitable ligands for Lewis-basic transition-metal fragments. Boron centered ligands may be roughly separated into three classes based on their level of saturation: boranes (I), boryl (II) and borylene (III) groups. II and III may additionally be subdivided into terminal and bridged ligands.[1–5] Here we concentrate on the first complex[6,7] with a bridging borylene ligand, **1** (see below), which has recently been investigated in an experimental electron-density (ED) study.[8,9] Analysis of the electron density of **1** by Bader's "quantum theory of atoms in molecules"[10] (QTAIM) suggested not only the absence of the direct Mn–Mn bond expected from the 18-valence-electron rule. It also indicated two "valence shell charge concentrations" (VSCCs) connecting the bridging boron atom to each of the two manganese

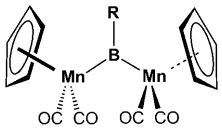


**1**: R = $C(CH_3)_3$
**2**: R = $N(CH_3)_2$

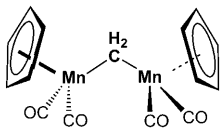


**4**

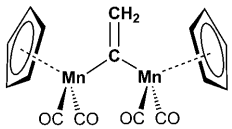


**3**

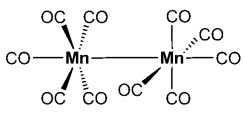


**5**

[a] K. Götz, Prof. Dr. M. Kaupp, Prof. Dr. H. Braunschweig
Institut für Anorganische Chemie, Universität Würzburg
Am Hubland, 97074 Würzburg (Germany)
Fax: (+49) 931-888-7135
E-mail: kaupp@mail.uni-wuerzburg.de

[b] Prof. Dr. D. Stalke
Institut für Anorganische Chemie, Universität Göttingen
Tammannstr. 4, 37077 Göttingen (Germany)

 © 2009 Wiley-VCH Verlag GmbH & Co. KGaA, Weinheim 

centers.[9] This is more consistent with a substituted borane than with the expected delocalized borylene description of the bridging ligand (analogous to bridging carbonyl ligands[11]).

Given the prototype nature of **1** as complex with a bridging boron ligand, and the somewhat unexpected results of the experimental QTAIM study (accompanied by computations at the BP86/TZVP level),[9] we provide here a systematic computational bonding comparison for **1** and its homologous amido-substituted complex **2**.[6,7,9,12,13] Furthermore, we extend the comparison to the closely related carbon-bridged complexes **3**[14] and **4**. Complex **3** represents the first methylene-bridged complex ever obtained,[15] and its early electron-density measurement has been interpreted to exhibit a direct Mn–Mn bond[16] Complex **4** in turn represents a related prototypical vinylidene-bridged complex. We systematically compare the electronic structure of these four bridged complexes, taking the unsupported dinuclear $Mn_2(CO)_{10}$ complex **5** as a reference with a direct Mn–Mn bond. We use various methods such as QTAIM, the electron-localization function (ELF[17,18]), and natural-population analyses (NPA[19]), based on density-functional calculations. Our aim is to answer the following questions:

a) Is there a direct metal–metal bond in any of the complexes **1**–**4**? For example, the methylene-bridged complex **3** has been taken as *the* prototypical example of a dimetallacyclopropane.[20] Is this appropriate? There has been substantial discussion of the question of metal–metal bonding in supported multinuclear carbonyl complexes,[21–25] also with bridging alkyne ligands,[26,27] and both QTAIM and ELF have been employed in this context.[11,26–36] We will include this in the discussion appropriately.
b) Is the bridging ligand in **1** or **2** a borylene with three valences, or does the bridge exhibit two well-defined localized two-center bonds, as suggested by the two VSCCs between the bridging boron and the two Mn atoms observed[9] experimentally for **1**? And what about the methylene and vinylidene bridges in **3** and **4**? It turns out that the interpretation of these questions depends in an unexpected way on the computational level (choice of exchange-correlation functional) employed, and we thus compare different methods.
c) Finally, we wish to compare the donation and back-donation from and to the bridging ligand for **1**–**4**, in the context of a classification of the binding ability of boron- versus carbon-centered bridging ligands,[37] and in view of the competition between bridge and direct metal–metal bonding.[11]

## Computational Details

All structure optimizations and harmonic frequency analyses were performed at the B3LYP/TZVP[38–42] level of theory using the Turbomole package[43–45] (versions 5.8 and 5.9). As starting point for the structure optimizations we used either coordinates from X-ray diffraction studies directly, or modified them to construct structural derivatives.

For the electronic structure analyses, subsequent single-point calculations were performed. In view of qualitative discrepancies of our B3LYP/TZVP data with the results of the experimental QTAIM study[9] (see below), we carried out further analyses with the gradient-corrected non-hybrid functionals BP86[46,47] and BLYP,[40,41,46,48] with the BHLYP hybrid functional[48] incorporating as much as 50% Hartree–Fock exchange, and at the Hartree-Fock (HF) level. Addition of an f-function for manganese (TZVPP basis) changed the results negligibly (data not reported). Also, structures optimized with the other functionals (BP86, BLYP, BHLYP) give almost the same QTAIM and ELF results (data not shown) as the B3LYP/TZVP structures, and we can thus restrict our discussion to the latter.

QTAIM analyses used the AIM2000[49] program package, whereas the ELF was analyzed and computed with a locally modified version of the TopMod program.[50,51] The ELF isosurfaces were visualized with the Molekel software.[52] Natural population analyses[19] were performed with Turbomole 5.9.

## Results and Discussion

**Optimized structures**: The recurring entity of the complexes **1**–**4** is the dicarbonyl-cyclopentadienyl manganese unit, which is related to the remaining organometallic fragment by a $C_2$-symmetry operation in the *trans* isomers studied. The well-studied reference compound **5** exhibits overall crystallographic $C_2$ symmetry, but the computations converge to a more symmetrical $D_{4d}$ structure. All computed distances and angles are within acceptable deviation of the available crystallographic data (within a few hundredths of an Å; only for **5** the deviations are somewhat larger), and the structures are confirmed as minima on the potential energy surface. The dimanganese decacarbonyl, **5**, is probably the paradigmatic example of an unsupported Mn–Mn single bond (but note that some 1–3 interactions have been discussed even in this case[11,32]). Its Mn–Mn bond length between 2.903 and 3.033 Å,[32,53,54] depending on the means of determination (see also Table 1), will be the reference value. Obviously, measured and optimized Mn–Mn distances of the bridged compounds **1** to **4**[6,13] are all significantly shorter and range from 2.806 to 2.857 Å. Together with the 18-valence-electron rule, this has been a main reason for the assumption of a direct metal–metal bond in these and related complexes.

### QTAIM analysis

**B3LYP/TZVP results**: Figure 1 provides molecular graphs and $\nabla^2\rho$ plots for **1**–**5** obtained with the B3LYP hybrid functional. We note first of all, that no "bond critical point" (BCP) and thus no bond path is found between the two Mn atoms for any of the bridged systems **1**–**4**, in contrast to the unsupported bond in reference complex **5**. The Mn–Mn midpoint is located in an area of positive $\nabla^2\rho$ and low $\rho$ in all bridged systems **1**–**4**. This agrees with the experimental results for **1**[9] and is consistent with the good bridging abilities of both borylene- and carbene-type ligands.

 © 2009 Wiley-VCH Verlag GmbH & Co. KGaA, Weinheim 

Table 1. Selected distances [Å] for the B3LYP/TZVP-optimized structures compared to experiment.

| Compound | | Theory | Experiment |
|---|---|---|---|
| **1** | Mn···Mn | 2.841 | 2.78190[a] |
| | $Mn-B_{bridge}$ | 2.037, 2.034 | 2.0215, 2.0206[a] |
| | B–C | 1.614 | 1.6092[a] |
| **2** | Mn···Mn | 2.857 | 2.790(6) |
| | $Mn-B_{bridge}$ | 2.047, 2.048 | 2.03, 2.03(6) |
| | B–N | 1.404 | 1.39(6) |
| **3** | Mn···Mn | 2.836 | 2.799(16) |
| | $Mn-C_{bridge}$ | 2.026, 2.025 | 2.026(16) |
| **4** | Mn···Mn | 2.806 | |
| | $Mn-C_{bridge}$ | 1.981 | |
| | $C_{bridge}=C$ | 1.326 | |
| **5** | Mn···Mn | 3.034 | 2.9042(32), 2.9078(54) |

[a] Supporting Information in ref. [9].

Table 2. BCP properties of selected bonds.

| Compound | Interaction | $\rho$ [e Å$^{-3}$] | $\nabla^2\rho$ [e Å$^{-5}$] |
|---|---|---|---|
| **1** | Mn–B | 0.658 | −0.004 |
| | | 0.662 | −0.004 |
| **2** | Mn–B | 0.642 | 0.158 |
| | | 0.640 | 0.165 |
| **3** | $Mn-C_{bridged}$ | 0.685 | 3.452 |
| | | 0.685 | 3.446 |
| **4** | $Mn-C_{bridged}$ | 0.739 | 4.155 |
| | | 0.739 | 4.171 |
| **5** | Mn–Mn | 0.160 | 0.119 |

It is a general observation in QTAIM analyses of (so far carbonyl- or alkyne-bridged) di- or oligonuclear carbonyl complexes[11,26,27,30] that direct metal–metal bonds compete with delocalized bonding via the bridge, and strong symmetrical bridges with good π-acceptor ligands tend to exclude direct M–M bonds (the same holds for results obtained with ELF[34,55]). The VSCCs associated with the bridged bond are connected to the bridging ligand in all cases. Delocalized bonding via the bridge dominates thus clearly over the direct Mn–Mn bonding in all of **1**–**4**, in contrast to **5**. The latter has a negative Laplacian at the BCP (which exists on the straight Mn–Mn connection line, compare Figure 1) but with a clear local maximum in $-\nabla^2\rho$, comparable to $F_2$[8] (see extensive discussion of the bonding in 5,[28,32,33,53,56] as reviewed also in ref. [11]). We will see below that the ELF analyses provide a similar picture. There have been arguments that weak M–M interactions may nevertheless be present but may not be identified using the standard instruments of QTAIM (but with alternative instruments like plots of total energy density or source functions, or orbital decomposition of the electron density).[26,27,29,35,36,57] Inspection[9] of the source function for **1** indicated strongly delocalized bonding, and the ratio $|V|/G$ was low. For the present discussion it suffices to note that bonding via the bridge dominates in all four cases, as the electrons from those metal d-orbitals potentially able to establish a direct Mn–Mn bond instead are delocalized mostly into the acceptor orbitals of the bridge. In this, the four ligands studied here resemble bridging carbonyl or alkyne ligands.[11,21–36] Note that the density topology in small ring systems may also be influenced by the core densities of the atoms in the perimeter.[58]

The bond paths between the bridging atom and the two Mn centers in **1** to **4** exhibit a pronounced inward curvature at the bridging atom. This is known to indicate bond delocalization[10] and is thought[59,60] to be related also to the donation of charge density from the bridge to the two metal centers. Near the Mn centers, the bond paths are almost linear. This cannot be taken to indicate low back donation, as the relevant Mn d-orbitals point anyhow largely into the direction of the bridging ligand. The values of $\rho(\mathbf{r}_{BCP})$ and $\nabla^2\rho(\mathbf{r}_{BCP})$ for these bonds are in all cases slightly asymmetric for the two Mn–B sides (no symmetry constraint was applied during the optimization). Borylene complex **2** has small negative $\nabla^2\rho$ values, complex **1** equally small positive ones at the BCPs. Both manganese–boron interactions may thus be taken as borderline cases between closed-shell dative and covalent shared bonding. The $M-C_{bridge}$ bonds in **3** and **4** exhibit comparable values of $\rho(\mathbf{r}_{BCP})$ and $\nabla^2\rho(\mathbf{r}_{BCP})$. The latter are positive, which would be consistent with more ionic Mn–C bonds in **3** and **4** than Mn–B bonds in **1** and **2** (see also below). We note in passing the expected,[11] relatively pronounced positive $\nabla^2\rho(\mathbf{r}_{BCP})$ values for terminal dative carbonyl metal-ligand interactions.

For the complexes **1**, **3**, and **4**, the B3LYP/TZVP calculations provide one VSCC near the bridging atom, pointing towards the Mn–Mn midpoint. This is similar to the QTAIM description of bridging carbonyl[11,30,31,56] and phosphane[55] ligands but clearly contradicts the experimental QTAIM results for **1**, which provided two B–Mn bond VSCCs, each one of them pointing from the bridging boron atom towards one of the Mn centers.[9] While the experimental study is thus more consistent with a description of the bridging ligand as a substituted borane, the B3LYP/TZVP picture is that of a delocalized three-center bond of a genuine borylene. Interestingly, the calculations do provide two B–Mn VSCCs for **2**. That is, the result already is in tune with the substituted-borane approach. However, the separation between the two attractors in $\nabla^2\rho$ is only marginal (see below). We will discuss below that the actual interpretation obtained by theory for **1**, **2**, and **4** depends remarkably on the computational level. At all levels, an additional VSCC is located between the bridging atom and each of its substituents (two in case of the $CH_2$ bridge in **3**).

In agreement with the experimental QTAIM study of **1**,[9] the valence shells of the metal atoms in **1** to **4** feature six VSCCs in an octahedral configuration with one of the edges of the octahedron pointing towards the cyclopentadienyl ligand. All other ligands face regions of charge depletion. This is interesting, as within QTAIM the cyclopentadienyl ligand behaves thus topologically as a single (six-electron) donor ligand. We note in passing that, in agreement with previous work,[11] eight VSCCs in a distorted cubic arrangement are found for each Mn atom in **5**.

 © 2009 Wiley-VCH Verlag GmbH & Co. KGaA, Weinheim 

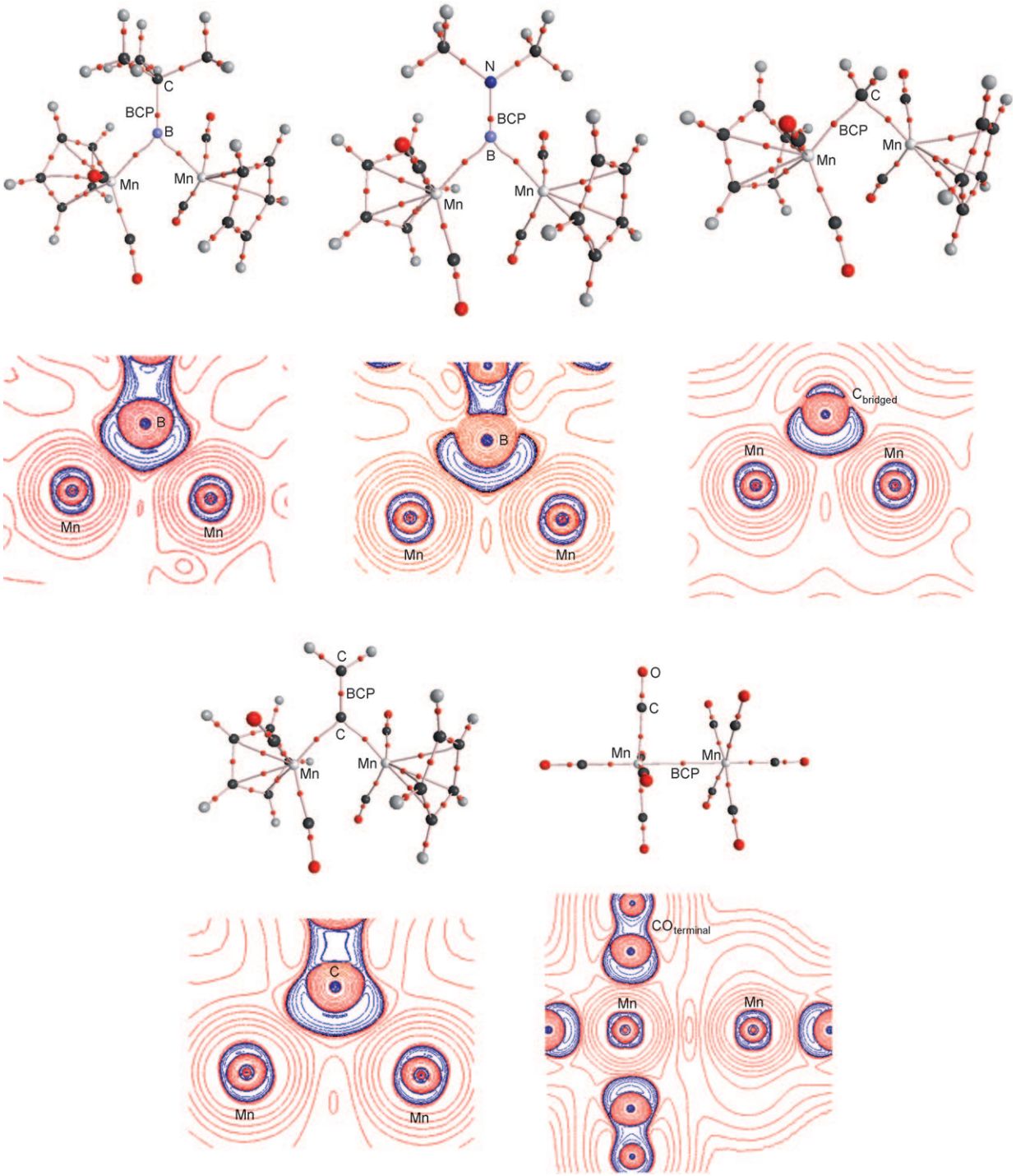


Figure 1. Molecular graphs and Laplacian maps; BCPs are indicated as red dots; charge accumulations ($\nabla^2\rho < 0$) are printed in blue (grey), charge depletions ($\nabla^2\rho > 0$) in red (black). B3LYP/TZVP results.

**Dependence on exchange-correlation functional**: Given the discrepancy between the number of computed (B3LYP/TZVP) and experimentally obtained B–Mn bonding VSCCs in **1**, we have compared charge densities obtained with different functionals (BP86,[46,47] BLYP,[40,41,46,48] B3LYP[38,40,41] and BHLYP[40,41,48]) and at the HF level. It is known that the local density approximation (LDA) and the generalized gradient approximation (GGA) tend to suffer from self-interaction errors and provide metal–ligand bonds in transition-metal complexes for which the covalent character is overestimated.[61–64] On the other hand, the semilocal exchange holes of GGA-type functionals like BP86 or BLYP are also thought to simulate non-dynamical correlation.[62,65] Hence, exact-exchange admixture renders the bonds more polar but

 © 2009 Wiley-VCH Verlag GmbH & Co. KGaA, Weinheim 

may also reduce the amount of non-dynamical correlation simulated. It should be noted that there is no clear preference in the literature for one type of functional when it comes to transition-metal systems. The above-mentioned balance between minimal self-interaction and adequate simulation of nondynamical correlation is difficult to achieve. While B3LYP is clearly the most popular functional in main group chemistry (albeit it also has been shown to exhibit severe shortcomings even in organic chemistry), it appears that the optimum amount of exact-exchange admixture varies for different systems and different properties (see, e.g., discussions in refs. [27,64,66–72]). B3LYP incorporates 20% and the BHLYP functional 50% HF exchange, and thus a comparison of these two hybrid functionals with the BP86 and BLYP GGA functionals should provide insight to an interrelation between charge transfer between metal and bridging ligand (and vice versa) and the computed features in $\nabla^2\rho$.

The number of VSCCs for Mn-$L_{bridge}$-Mn bonding depends on this exact-exchange admixture for all bridged complexes but **3** (Table 3). At all levels, the latter methylene-bridged complex exhibits only one VSCC, consistent with the delocalized three-center bonding picture that is common also for bridging carbonyl ligands.[11,30,31,56] In contrast, with GGA functionals (BP86, BLYP), complexes **1** and **4** feature two VSCCs and thus a localized two-center bonding picture. Exact-exchange admixture changes this to a delocalized picture with one VSCC already at B3LYP level (and also with 50% exact exchange at BHLYP level). Finally, the amido-substituted borylene complex **2** has two VSCCs at B3LYP and BLYP, BP86 levels, and switches to one VSCC only at BHLYP level (pure HF results give the same qualitative topology as BHLYP for all complexes; data not shown). In all bridged complexes except **3**, the Laplacian distribution near the bridging ligand appears thus borderline between one and two VSCCs, thereby explaining the unusual dependence on the exchange-correlation functional. Apparently the nuclear configurations of complexes **1**, **2**, and **4** are close to a catastrophe point within Bader's topological theory of molecular structure, indicating a borderline between two topologically different bonding situations.[10,73] A somewhat related situation has very recently been observed for the Co-($C_2$) QTAIM bond topology in an alkyne-bridged dicobalt complex, where either one or two Co–C bond paths were obtained, with qualitative differences even between closely similar, crystallographically independent molecules.[26] The topologically unstable situation was attributed to a very shallow density distribution in the Co-($C_2$) triangles marking the interactions between the two cobalt centers and the bridging alkyne ligand, and it was argued that discrepancies may well be caused by measurement errors or artefacts in the multipole refinement of the experimental charge density.[26] As shown here, a bifurcating bonding situation may also cause a high sensitivity to the computational level.

The visualization as a contour plot of $\nabla^2\rho$ (Figure 2) indicates, that the splitting into two VSCCs at BP86 or BLYP level for **1** (and also for **4**; data not shown) is not very pronounced, certainly less so than suggested by the experimental Laplace map for **1**[9] (see footnote [b] to Table 3; note that the experimental density distribution around boron is also more asymmetric than computationally suggested). This is confirmed by the values of $\nabla^2\rho$ given in Table 3: In those cases where a splitting into two VSCCs occurs (**1**, **2**, and **4** with BLYP and BP86, and additionally **2** with B3LYP), the separatice $\nabla^2\rho$ values are only slightly less negative than the attractor with the lower $|\nabla^2\rho|$ value. For **1** and **4**, the separatice value is only about 0.02–0.06 e Å$^{-5}$ or 0.2–0.7% below the attractor value (separation is somewhat clearer with BP86 than with BLYP), compared to more than 1.6 e Å$^{-5}$ or 25% determined experimentally (footnote [b] to Table 3). The separation is more pronounced for **2** with GGA functionals (about 6–7% for BLYP and BP86) but becomes less with the B3LYP hybrid functional (1.2%), compare Table 3.

As we move from BHLYP to B3LYP to BP86 or BLYP, we notice furthermore that the overall region of negative $\nabla^2\rho$ becomes wider and more distinct (Figure 2), indicating the expected enhanced covalency at GGA level. We note also that, as the two VSCCs present at GGA level merge into one VSCC at hybrid level, the $\nabla^2\rho$ value at the attractor of the corresponding merged basin is more negative than those at the two previously separate attractors (Table 3). Additionally, increased exact-exchange admixture renders $\nabla^2\rho$ at the single attractor more negative even for **3**, while the qualitative topology remains unchanged. We may generalize these observations by stating that exact-exchange admixture in the hybrid functionals accumulates charge in the region below the bridging atom pointing towards the Mn···Mn midpoint, at the expense of the regions close to the direct Mn-bridge connection lines.

On the other hand, a change in the number of VSCCs with different functionals is not accompanied by large changes in the BCP properties $\rho(\mathbf{r}_{BCP})$ and $\nabla^2\rho(\mathbf{r}_{BCP})$. These respond marginally, with a slightly more positive $\nabla^2\rho(\mathbf{r}_{BCP})$

Table 3. Number of attractors in $-\nabla^2\rho$, with $\nabla^2\rho$ values, and separatice $\nabla^2\rho$ values [e Å$^{-5}$] for the di- or trisynaptic VSCCs at the bridge.[a]

| VSCC $\nabla^2\rho$ values | | BP86 | BLYP | B3LYP | BHLYP |
|---|---|---|---|---|---|
| 1[b] | separative | *2*: −5.561,−5.359 | *2*: −5.896, −5.683 | *1*: −6.287 | *1*: −7.554 |
| | attractor | −5.324 | −5.663 | | |
| 2 | separative | *2*: −5.247, −5.226 | *2*: −5.566, −5.546 | *2*: −5.769, −5.788 | *1*: −6.871 |
| | attractor | −4.872 | −5.218 | −5.699 | |
| 3 | separative | | | | |
| | attractor | *1*: −14.863 | *1*: −15.740 | *1*: −16.639 | *1*: −18.973 |
| 4 | separative | *2*: −16.466, −16.478 | *2*: −17.210, −17.222 | *1*: −18.281 | *1*: −20.757 |
| | attractor | −16.406 | −17.178 | | |

[a] At B3LYP/TZVP structures. Number of attractors in bold italics. [b] Experimentally determined values for 1 are:[9] −7.493 e Å$^{-5}$ and −6.566 e Å$^{-5}$ for the two VSCCs and −4.868 e Å$^{-5}$ for the separative.

 © 2009 Wiley-VCH Verlag GmbH & Co. KGaA, Weinheim 

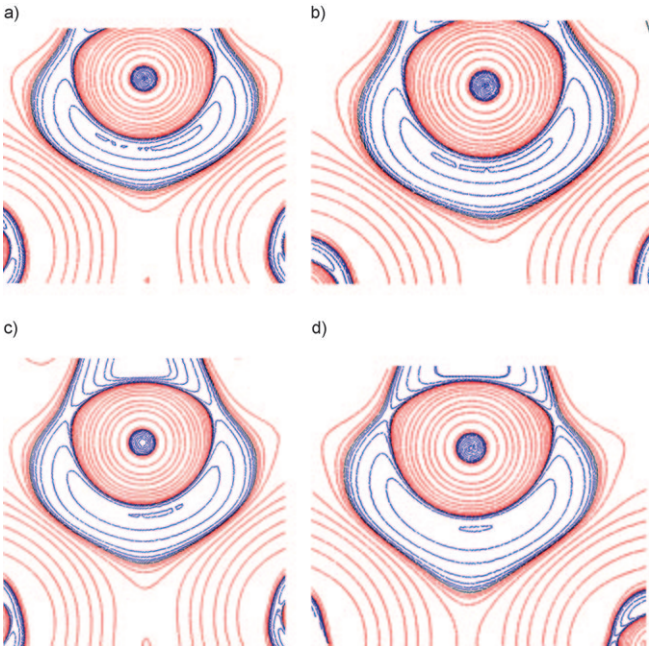


Figure 2. Contour plots of $\nabla^2\rho$ for **1** with different exchange-correlation functionals; values for the most negative contour a) BP86: −5.302 Å, b) BLYP: −5.591 Å, c) B3LYP: −6.169 Å, d) BHLYP: −7.422 Å (the area around bridgehead atom is shown).

value upon increasing exact-exchange admixture, consistent with the above-mentioned more ionic metal-ligand bonding. Finally, it is worth mentioning, that at none of the computational levels employed, a Mn–Mn BCP appears for any of the four complexes **1**–**4**.

To what extent is the change in the topology of the charge density with the functional related to charge transfer from and to the bridging ligand? Table 4 summarizes NPA charges for the bridge and the metal fragments, as well as for Mn and the bridging atom, in **1** to **4**, comparing different functionals. We note first a pronounced inequivalence of the two metal fragments for **1**, in contrast to the other three complexes. This is related to the conformation of the alkyl substituent on boron. In case of the two boron complexes **1** and **2**, there is moderate yet notable net charge transfer from the bridging ligand to the two $MnCp(CO)_2$ moieties. This contrasts with the methylene and vinylidene complexes **3** and **4**, where charge transfer of similar magnitude occurs *to* the bridge. These observations are consistent with the more pronounced curvatures of the L–Mn bond paths at the bridging atom for **1** and **2** compared to **3** and **4** (cf. Figure 1): Significant donation from the bridge to the metal fragments is expected to enhance the curvature.[11,59,60]

The lower electronegativity of B versus C is particularly notable from the charge of the bridging atom itself, which is appreciably positive for **1** and **2**, strongly negative for **3** and weakly negative for **4**, reflecting charge distributions within the various bridging ligands, as well as the donation/back-donation between bridging ligand and metal fragments. With the exception of **3**, the Mn centers themselves exhibit

Table 4. NPA charges for atoms and molecular fragments.[a]

| | | BLYP | B3LYP | BHLYP |
|---|---|---|---|---|
| 1 | Mn1[b] | −0.395 | −0.397 | −0.345 |
| | Mn2[b] | −0.385 | −0.386 | −0.331 |
| | B[b] | 0.752 | 0.780 | 0.800 |
| | $MnCp(CO)_2$ 1 | −0.146 | −0.156 | −0.160 |
| | $MnCp(CO)_2$ 2 | −0.078 | −0.085 | −0.089 |
| | B(*t*Bu) ligand | 0.224 | 0.241 | 0.249 |
| 2 | Mn[c] | −0.355 | −0.352 | −0.295 |
| | B | 0.683 | 0.705 | 0.724 |
| | $MnCp(CO)_2$[c] | −0.114 | −0.116 | −0.111 |
| | $B(NMe_2)$ ligand | 0.228 | 0.231 | 0.222 |
| 3 | Mn[c] | 0.058 | 0.058 | 0.056 |
| | C | −0.529 | −0.541 | −0.561 |
| | $MnCp(CO)_2$[c] | 0.093 | 0.100 | 0.114 |
| | $CH_2$ ligand | -0.187 | −0.200 | −0.227 |
| 4 | Mn[c] | −0.217 | −0.220 | −0.223 |
| | C | −0.034 | −0.038 | −0.056 |
| | $MnCp(CO)_2$[c] | 0.181 | 0.121 | 0.127 |
| | $CH_2$=C ligand | −0.237 | −0.242 | −0.255 |

[a] Functional/TZVP//B3LYP/TZVP results. [b] Experimental QTAIM charges for 1[9] are −0.73 and −0.76 e for the two Mn atoms, +1.04 e for B, and overall +0.69 e for the bridging ligand. [c] Averaged over both $MnCp(CO)_2$ fragments.

negative partial charges, most significantly for the boron complexes **1** and **2** (Table 4). The extensive backbonding in **3** (and the resulting slightly positive charge on Mn) has already been discussed previously as origin of the high stability of the methylene-bridged complex[20,74] (albeit under the pretext of a metallacyclopropane topology with direct M–M bond). Bridging carbene ligands are of potential interest in catalysis and various applications, and their extent of donation/back-donation has therefore been under extensive discussion.[75] Bridging boron ligands have been rarely studied, and therefore their bonding is of current interest. The charges in Table 4 suggest that a) the significant thermochemical stability of bridged borylene complexes[13] may derive partly from electrostatic contributions (cf. fragment charges of **1** and **2**), and b) the appreciably positive charge at boron explains the accessibility towards nucleophilic attack at the bridging ligand.[12,76–78]

Turning to the dependence on the functional (Table 4), we see more charge transfer from the bridge to the metal fragments for the boron complexes **1** and **2** with increasing exact-exchange admixture from BLYP to B3LYP to BHLYP (with the exception of the BHLYP result for **2**, which is lower, for as yet unknown reasons). That is, the enhanced "localization" of charge with exact-exchange admixture works from the bridge to the metal. The situation is reversed for the carbon-bridged complexes **3** and **4**, where the net charge transfer *to* the bridge increases with increasing exact exchange. All four systems have thus in common that the overall charge transfer is enhanced with exact-exchange admixture, but the direction differs between boron and carbon ligands.

The experimentally obtained QTAIM charges for **1**[9] indicate even more charge transfer from the bridging ligand to the Mn centers (cf. footnote [b] in Table 4). This larger bond

 © 2009 Wiley-VCH Verlag GmbH & Co. KGaA, Weinheim 

polarity is well in line with previous comparisons between QTAIM and NPA charges.[19]

**ELF analysis**: The electron-localization function (ELF[17,18]) provides an alternative real-space function for the analysis of non-trivial bonding situations. While the ELF exhibits certain similarities to the negative of $\nabla^2\rho$ in terms of topological analysis,[79] it differs from the latter in a number of points, for example, in the precise position of the attractors or in the number of attractors for covalent bonds.[80] The ELF has an extensive history of application to transition metal systems (see, e.g., reviews in refs. [18,81]), including questions of metal–metal bonding in polynuclear carbonyl and related clusters.[34,82–87] For example, the ELF shows no direct M–M bonding attractors for the triscarbonyl-bridged Fe–Fe interaction in $[Fe_2(CO)_9]$[34] or for the bridged edge in the $C_{2v}$ isomer of $[Fe_3(CO)_{12}]$,[87] in both cases yielding conclusions consistent with the QTAIM results (as another example, no direct Rh–Rh bonding attractors are found on the carbonyl-bridged faces of $[Rh_6(CO)_{16}]$[34]). The topological discussion of the ELF is typically based on the synaptic order of its attractors and the associated basins,[88,89] where monosynaptic valence attractors are assigned to lone pairs, disynaptic attractors to two-center bonds, and attractors of higher synapticity to delocalized multicenter bonding.

Consistent with the QTAIM results above, none of the bridged complexes **1** to **4** exhibits a direct Mn–Mn bonding attractor (cf. Figure 3), in contrast to the unsupported complex **5**, which exhibits a disynaptic bonding attractor at an ELF value of 0.42. The delocalized Mn-bridge-Mn bonding is apparent from the saddle-shaped areas of the ELF = 0.7 isosurfaces in Figure 3. Interestingly, further increase of the isosurface value reveals in some cases the separation into different attractors with associated basins in ELF, dependent again on the exchange-correlation functional.

The trends in this case are closely consistent with the behavior of the VSCCs in the density, as discussed above: At BHLYP hybrid level with 50% HF exchange, only one trisynaptic attractor with ELF values near 0.82–0.88 is observed in all cases **1**–**4** (cf. Table 5). It points towards the Mn···Mn midpoint, as is the case for the corresponding VSCC. Consistent with the discussion for $-\nabla^2\rho$ (cf. Figures 1 and 2), a decrease of exact-exchange admixture tends to diminish the high-ELF area in this trisynaptic domain and creates high-ELF attractors close to the connection line between Mn and the bridging atom. While no further attractors are found for the methylene-bridged complex **3** at any level (Table 5), already at B3LYP level complex **2** develops two disynaptic attractors in addition to the central trisynaptic attractor. This is also the case for **1**, albeit in a less pronounced fashion (the two disynaptic attractors and their basins are clearly nonequivalent). In case of **4**, the B3LYP results exhibit only the trisynaptic attractor, whereas two disynaptic attractors appear additionally at BLYP level. This behavior is consis-

Table 5. Number of trisynaptic (*disynaptic*) ELF attractors associated with the bridge–Mn bond; dependence on the functional.

| Compound | BLYP | B3LYP | BHLYP |
|---|---|---|---|
| **1** | 1 (2) | 1 (2) | 1 (0) |
| **2** | 1 (2) | 1 (2) | 1 (0) |
| **3** | 1 (0) | 1 (0) | 1 (0) |
| **4** | 1 (2) | 1 (0) | 1 (0) |

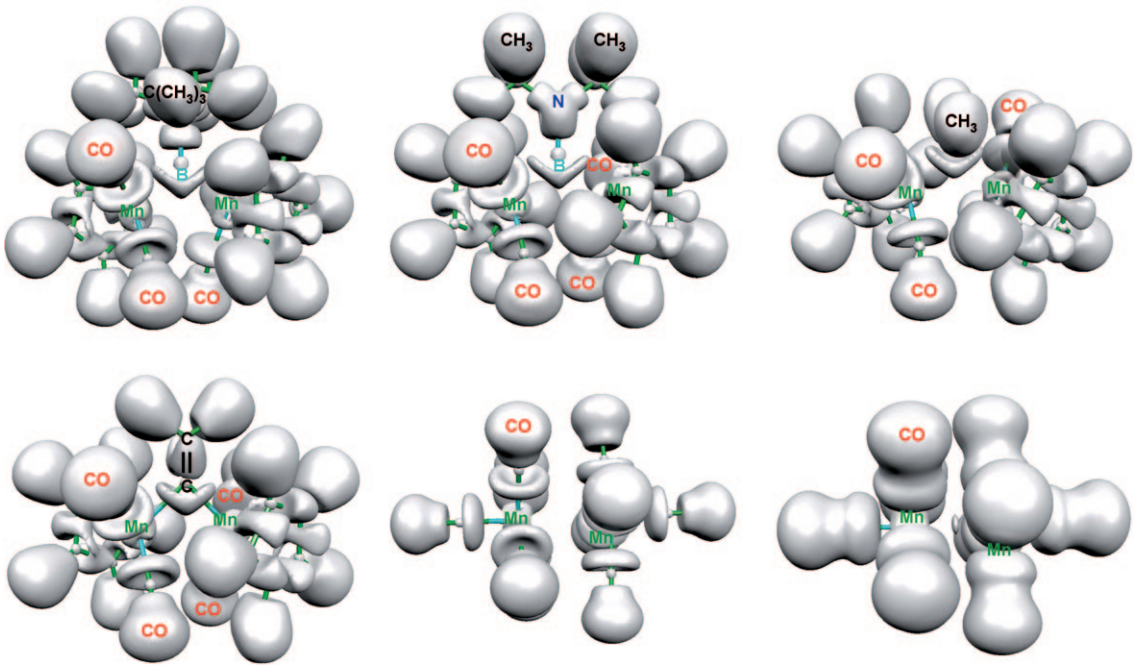


Figure 3. ELF isosurface plots; B3LYP/TZVP results; ELF = 0.7 isosurfaces, unless noted otherwise.

 © 2009 Wiley-VCH Verlag GmbH & Co. KGaA, Weinheim 

tent with the pronounced bond covalency at GGA level and enhanced charge transfer to or from the bridge discussed above. The overall trends in $-\nabla^2\rho$ and ELF are thus very similar (wider areas of very negative $\nabla^2\rho$ and high positive ELF values at GGA vs hybrid level). However, the development of disynaptic VSCCs in the density destroys the trisynaptic ones, whereas the trisynaptic ELF attractors survive even when the disynaptic ones appear. Again, we see close similarity but subtle differences between these two quantities. As for the density, the di- and trisynaptic ELF basins at GGA (BLYP) level tend to be separated only little. To give just one example, the ELF values at the tri- and disynaptic attractors for **2** (BLYP data) are 0.815 and 0.830, respectively, whereas the separative (merging of the three domains) is at ELF = 0.806 (in contrast, the single trisynaptic attractor at BHLYP level is at ELF = 0.883). Thus we conclude that the ELF for these systems (except for **3**) is close to a bifurcation point between two different bonding topologies, just as observed for $-\nabla^2\rho$. This explains again the extreme sensitivity to the computational level, notably to the exchange-correlation functional.

The Mn valence regions are characterized by an approximately octahedral distribution of ELF attractors, similar to the arrangement of the VSCCs around the metal centers in the QTAIM analysis (cf. Figure 4 for a comparison).[80] As had been noted previously,[34] the non-bonding valence localization regions around coordinated metal centers tend to be arranged in the form of a dual polyhedron with respect to the ligand framework.

Figure 4. VSCCs in $-\nabla^2\rho$ (purple/black) mapped on ELF distribution (isosurface ELF = 0.73 in grey) around an Mn atom in **4**.

## Conclusion

Both QTAIM and ELF analyses of the borylene-bridged complex **1** confirm the absence of significant direct Mn–Mn bonding (question a in the introduction), as had been suggested by the experimental charge density study. Indeed, in none of the systems studied here we find any QTAIM or ELF evidence for a direct Mn–Mn bond. This is most remarkable for the methylene complex **3** (and probably also for the vinylidene complex **4**), because this was often taken as the prototype of a dimetallacyclopropane. All four bridging ligands in our title systems **1**–**4** may serve as good to excellent π-acceptors towards the $MnCp(CO)_2$ organometallic moieties. Charge transfer from metal-metal-bonding MOs into empty orbitals on the bridge provides a mechanism for preventing the direct Mn–Mn bond. The two residues are thus held together mainly by delocalized bonding across the bridging ligand, consistent with previous analyses for carbonyl complexes (see, for example, ref.[11] and papers cited therein). The consistency between the descriptions by QTAIM and ELF is remarkable, because the ELF has a different connection to electron pairing and localization (and to the Pauli principle) than $-\nabla^2\rho$ and thus provides a complementary independent approach.

Unexpected behavior has been found for the synapticity of the VSCCs and of the ELF attractors for the bridge in **1**–**4**. The methylene complex **3** exhibits the most clear-cut situation. A Mn-C-Mn three-center bonding picture is obtained at all computational levels, with only one VSCC or ELF basin associated with the bridgehead. We have found a striking qualitative dependence on the exchange-correlation functional in DFT calculations for the remaining bridged complexes **1**, **2**, and **4**: Depending on the exact-exchange admixture in the functional, the two boron bridges in **1** and **2** and the vinylidene bridge in **4** may involve delocalized three-center bonding across the bridge (as indicated by only one VSCC or by one trisynaptic ELF attractor) or separate into two two-center bonds (two VSCCs or overall three ELF attractors). GGA-type functionals like BP86 and BLYP favor a separation, whereas exact-exchange admixture in hybrid functionals like B3LYP or BHLYP shifts matters increasingly into a three-center bonding situation by accumulating charge in the area between the bridging atom and the Mn···Mn midpoint. Thus, for **1**, BP86 or BLYP calculations agree qualitatively with the recent experimental charge density study by exhibiting two separated VSCCs (as well as two disynaptic and one trisynaptic ELF basins). In contrast, hybrid functionals collapse these basins (one VSCC in $-\nabla^2\rho$, one trisynaptic ELF basin). In these complexes, we are close to bifurcation points in both $-\nabla^2\rho$ and ELF, and slightly altered charge transfer from or to the bridge may switch matters from one to the other bonding situation. We should note, however, that the separation between the two VSCCs in **1** even at GGA level is much less pronounced than found by the experimental charge density analysis. Of course we cannot disregard the role of the multipole expansion in the experimental determinations. At this stage, we cannot even recommend a preferred functional. Question b in the introduction remains thus open both theoretically and experimentally. Further work on comparable nontrivial bonding situations should be rewarding, both by experimental electron density studies and by computations.

Comparing finally the boron- and carbon-bridged complexes in this study (question c in the Introduction), the main difference is the net charge transfer *from* the bridge to the two Mn atoms in the borylene complexes **1** and **2** compared to the net charge transfer *to* the bridge in the methylene and vinylidene bridged complexes **3** and **4**. This reflects the overall better donor and diminished acceptor capabilities of borylene compared to carbene ligands as bridging units in this context. A positive charge at boron explains fur-

 © 2009 Wiley-VCH Verlag GmbH & Co. KGaA, Weinheim 

thermore the accessibility to attack by nucleophiles at the bridging atom.

## Acknowledgements

This work has been supported by DFG priority programme 1178 ("Experimental determination of electron density"). K.G. acknowledges a PhD scholarship by Fonds der chemischen Industrie. We thank R. Dewhurst and M. Burzler for helpful discussions.

[1] H. Braunschweig, *Angew. Chem.* **1998**, *110*, 1882; *Angew. Chem. Int. Ed.* **1998**, *37*, 1786.
[2] H. Braunschweig, C. Kollann, D. Rais, *Angew. Chem.* **2006**, *118*, 5380; *Angew. Chem. Int. Ed.* **2006**, *45*, 5254.
[3] H. Braunschweig, M. Colling, *Coord. Chem. Rev.* **2001**, *223*, 1.
[4] S. Aldridge, D. L. Coombs, *Coord. Chem. Rev.* **2004**, *248*, 535.
[5] G. J. Irvine, M. J. G. Lesley, T. B. Marder, N. C. Norman, C. R. Rice, E. G. Robins, W. R. Roper, G. R. Whittell, L. J. Wright, *Chem. Rev.* **1998**, *98*, 2685.
[6] H. Braunschweig, T. Wagner, *Angew. Chem.* **1995**, *107*, 904; *Angew. Chem. Int. Ed. Engl.* **1995**, *34*, 825.
[7] H. Braunschweig, B. Ganter, *J. Organomet. Chem.* **1997**, *545*, 163.
[8] R. F. W. Bader, H. Essen, *J. Chem. Phys.* **1984**, *80*, 1943.
[9] U. Flierler, M. Burzler, D. Leusser, J. Henn, H. Ott, H. Braunschweig, D. Stalke, *Angew. Chem.* **2008**, *120*, 4393; *Angew. Chem. Int. Ed.* **2008**, *47*, 4321.
[10] R. W. F. Bader, *Atoms in Molecules: A Quantum Theory*, Oxford University Press, Oxford, **1990**.
[11] P. Macchi, A. Sironi, *Coord. Chem. Rev.* **2003**, *238–238*, 383.
[12] H. Braunschweig, M. Müller, *Chem. Ber.* **1997**, *130*, 1295.
[13] H. Braunschweig, C. Burschka, M. Burzler, S. Metz, K. Radacki, *Angew. Chem.* **2006**, *118*, 4458; *Angew. Chem. Int. Ed.* **2006**, *45*, 4352.
[14] K. Folting, J. C. Huffman, L. N. Lewis, K. Caulton, *Inorg. Chem.* **1979**, *18*, 3483.
[15] W. A. Herrmann, B. Reiter, H. Biersack, *J. Organomet. Chem.* **1975**, *97*, 245.
[16] D. A. Clemente, B. Rees, G. Bandoli, M. C. Biagini, B. Rieter, W. A. Herrmann, *Angew. Chem.* **1981**, *93*, 920; *Angew. Chem. Int. Ed. Engl.* **1981**, *20*, 887.
[17] A. D. Becke, K. E. Edgecombe, *J. Chem. Phys.* **1990**, *92*, 5397.
[18] A. Savin, R. Nesper, S. Wengert, T. F. Fässler, *Angew. Chem.* **1997**, *109*, 1892; *Angew. Chem. Int. Ed. Engl.* **1997**, *36*, 1809.
[19] A. E. Reed, R. B. Weinstock, F. Weinhold, *J. Chem. Phys.* **1985**, *83*, 735.
[20] D. C. Calabro, D. L. Lichtenberger, W. A. Herrmann, *J. Am. Chem. Soc.* **1981**, *103*, 6852.
[21] J. W. Lauher, M. Elian, R. H. Summerville, R. Hoffmann, *J. Am. Chem. Soc.* **1976**, *98*, 3219.
[22] D. L. Thorne, R. Hoffmann, *Inorg. Chem.* **1978**, *17*, 126.
[23] R. Hoffmann, R. H. Summerville, *J. Am. Chem. Soc.* **1979**, *101*, 3821.
[24] S. Shaik, R. Hoffmann, C. R. Fisel, R. H. Summerville, *J. Am. Chem. Soc.* **1980**, *102*, 4556.
[25] H. Willem, E. J. Baerends, P. Ros, *Faraday Symp.* **1980**, *14*, 211.
[26] J. Overgaard, H. F. Clausen, J. A. Platts, B. B. Iversen, *J. Am. Chem. Soc.* **2008**, *130*, 3834.
[27] J. A. Platts, G. J. S. Evans, M. P. Coogan, J. Overgaard, *Inorg. Chem.* **2007**, *46*, 6291.
[28] P. Macchi, D. M. Prosperpio, A. Sironi, *J. Am. Chem. Soc.* **1998**, *120*, 13429.
[29] A. A. Low, K. L. Kunze, P. J. MacDougall, M. B. Hall, *Inorg. Chem.* **1991**, *30*, 1079.
[30] P. Macchi, L. Garlaschelli, A. Sironi, *J. Am. Chem. Soc.* **2002**, *124*, 14173.
[31] P. Macchi, L. Garlaschelli, S. Martinengo, A. Sironi, *J. Am. Chem. Soc.* **1999**, *121*, 10428.
[32] R. Bianchi, G. Gervasio, D. Marabello, *Inorg. Chem.* **2000**, *39*, 2360.
[33] G. Gervasio, R. Bianchi, D. Marabello, *Chem. Phys. Lett.* **2004**, *387*, 481.
[34] M. Kaupp, *Chem. Ber.* **1996**, *129*, 527.
[35] M. Finger, J. Reinhold, *Inorg. Chem.* **2003**, *42*, 8128.
[36] E. Hunstock, C. Mealli, M. J. Calhorda, J. Reinhold, *Inorg. Chem.* **1999**, *38*, 5053.
[37] A. W. Ehlers, E. J. Baerends, F. M. Bickelhaupt, U. Radius, *Chem. Eur. J.* **1998**, *4*, 210.
[38] A. D. Becke, *J. Chem. Phys.* **1993**, *98*, 5648.
[39] P. J. Stephens, F. J. Devlin, C. F. Chabalowski, M. J. Frisch, *J. Phys. Chem.* **1994**, *98*, 11623.
[40] C. Lee, W. Yang, R. G. Parr, *Phys. Rev. B* **1988**, *37*, 785.
[41] B. Miehlich, A. Savin, H. Stoll, H. Preuss, *Chem. Phys. Lett.* **1989**, *157*, 200.
[42] A. Schäfer, C. Huber, R. Ahlrichs, *J. Chem. Phys.* **1994**, *100*, 5829.
[43] R. Ahlrichs, M. Bär, M. Häser, H. Horn, C. Kölmel, *Chem. Phys. Lett.* **1989**, *162*, 165.
[44] O. Treutler, R. Ahlrichs, *J. Chem. Phys.* **1995**, *102*, 346.
[45] M. v. Arnim, R. Ahlrichs, *J. Comput. Chem.* **1998**, *19*, 1746.
[46] A. D. Becke, *Phys. Rev. A* **1998**, *38*, 3098.
[47] J. P. Perdew, *Phys. Rev. B* **1986**, *33*, 8822.
[48] A. D. Becke, *J. Chem. Phys.* **1993**, *98*, 1372.
[49] F. Biegler-König, J. Schönbohm, *J. Comput. Chem.* **2002**, *23*, 1489.
[50] S. Noury, X. Krokidis, F. Fuster, B. Silvi, *ToPMoD input Manual*, Paris (France), **1997**.
[51] S. Noury, X. Krokidis, F. Fuster, B. Silvi, *Comput. Chem.* **1999**, *23*, 597.
[52] P. Flükiger, H. P. Lüthi, S. Portmann, J. Weber, in *Swiss National Supercomputing Centre CSCS*, Swiss National Supercomputing Centre CSCS, Manno (Switzerland), **2000**.
[53] R. Bianchi, G. Gervasio, D. Marabello, *Chem. Commun.* **1998**, 1535.
[54] L. J. Farrugia, P. R. Mallinson, B. Stewart, *Acta Crystallogr. Sect. B* **2003**, *59*, 234.
[55] S. Schinzel, M. Kaupp, unpublished results.
[56] C. Bo, J.-P. Sarasa, J. M. Poblet, *J. Phys. Chem.* **1993**, *97*, 6362.
[57] C. Gatti, D. Lasi, *Faraday Discuss.* **2007**, *135*, 55.
[58] J. Henn, D. Leusser, D. Stalke, *J. Comput. Chem.* **2007**, *28*, 2317.
[59] P. Macchi, D. M. Prosperpio, A. Sironi, *J. Am. Chem. Soc.* **1998**, *120*, 1447.
[60] W. Scherer, G. Eickerling, D. Shorokhov, E. Gullo, S. G. McGrady, P. Sirsch, *New J. Chem.* **2006**, *30*, 309.
[61] S. Patchkovskii, T. Ziegler, *J. Chem. Phys.* **1999**, *111*, 5730.
[62] W. Koch, M. C. Holthausen, *A Chemist's Guide to Density Functional Theory: An Introduction*, Wiley-VCH, Weinheim, **2000**.
[63] M. Kaupp, R. Reviakine, O. L. Malkina, A. Arbuznikov, B. Schimmelpfennig, V. G. Malkin, *J. Comput. Chem.* **2002**, *23*, 794.
[64] M. Munzarova, M. Kaupp, *J. Phys. Chem. A* **1999**, *103*, 9966.
[65] J. P. Perdew, M. Ernzerhof, K. Burke, *J. Chem. Phys.* **1996**, *105*, 9982.
[66] J. Fritscher, P. Hrobarik, M. Kaupp, *J. Chem. Phys. B* **2007**, *111*, 4616.
[67] M. Kaupp, R. Reviakine, O. L. Malkina, A. V. Arbouznikov, B. Schimmelpfennig, V. G. Malkin, *J. Comput. Chem.* **2002**, *23*, 794.
[68] C. Remenyi, R. Reviakine, M. Kaupp, *J. Phys. Chem. B* **2007**, *111*, 8290.
[69] F. Furche, J. P. Perdew, *J. Chem. Phys.* **2006**, *124*, 044103.
[70] W. Koch, M. C. Holthausen, *A Chemist's Guide to Density Functional Theory*, 2nd ed., Wiley-VCH, Weinheim, **2001**.
[71] S. Riedel, M. Kaupp, *Inorg. Chem.* **2006**, *45*, 1228.
[72] S. Riedel, M. Straka, M. Kaupp, *Phys. Chem. Chem. Phys.* **2004**, *6*, 1122.
[73] R. F. W. Bader, T. T. Nguyen-Dang, Y. Tal, *Rep. Prog. Phys.* **1981**, *44*, 893.
[74] P. Hofmann, *Angew. Chem.* **1979**, *91*, 591; *Angew. Chem. Int. Ed. Engl.* **1979**, *18*, 554.

 © 2009 Wiley-VCH Verlag GmbH & Co. KGaA, Weinheim 

[75] K. H. Döth, H. Fischer, P. Hofmann, F. R. Kreissl, U. Schubert, K. Weiss, *Transition Metal Carbene Complexes*, Verlag Chemie, Weinheim, **1983**.
[76] H. Braunschweig, M. Colling, *J. Organomet. Chem.* **2000**, *614–615*, 18.
[77] H. Braunschweig, M. Colling, C. Hu, *Inorg. Chem.* **2003**, *42*, 941.
[78] H. Braunschweig, M. Colling, C. Hu, K. Radacki, *Inorg. Chim. Acta* **2004**, *357*, 1822.
[79] R. F. W. Bader, S. Johnson, T. H. Tang, P. L. A. Popelier, *J. Phys. Chem.* **1996**, *100*, 15398.
[80] R. W. F. Bader, G. L. Heard, *J. Chem. Phys.* **1999**, *111*, 8789.
[81] B. Silvi, J. Pilme, F. Fuster, M. E. Alikhani, *NATO Science Series, II: Mathematics, Phys. Chem.* **2003**, *116*, 241.
[82] K. Besancon, G. Laurenczy, T. Lumini, R. Roulet, R. Bruyndonckx, C. Daul, *Inorg. Chem.* **1998**, *37*, 5634.
[83] H. Chevreau, C. Martinsky, A. Sevin, C. Minot, B. Silvi, *New J. Chem.* **2003**, *27*, 1049.
[84] U. Effertz, U. Englert, F. Podewils, A. Salzer, T. Wagner, M. Kaupp, *Organometallics* **2003**, *22*, 264.
[85] G. Jansen, M. Schubart, B. Findeis, L. H. Gade, I. J. Scowen, M. McPartlin, *J. Am. Chem. Soc.* **1998**, *120*, 7239.
[86] P. J. Low, R. Rousseau, P. Lam, K. A. Udachin, G. D. Enright, J. S. Tse, D. D. M. Wayner, A. J. Carty, *Organometallics* **1999**, *18*, 3885.
[87] J. Andres, S. Berski, M. Feliz, R. Llusar, F. Sensato, B. Silvi, *Comptes Rendus Chimie* **2005**, *8*, 1400.
[88] A. Savin, B. Silvi, F. Colonna, *Can. J. Chem.* **1996**, *74*, 1088.
[89] B. Silvi, A. Savin, *Nature* **1994**, *371*, 683.

Received: June 3, 2008
Published online: November 28, 2008

 © 2009 Wiley-VCH Verlag GmbH & Co. KGaA, Weinheim 